Published in final edited form as:
Cell Metab. 2010 March 3; 11(3): 194–205. doi:10.1016/j.cmet.2010.02.003.

The G_0/G_1 Switch Gene 2 Regulates Adipose Lipolysis through Association with Adipose Triglyceride Lipase

Xingyuan Yang[1,2], **Xin Lu**[1,2], **Marc Lombès**[5], **Geun Bae Rha**[3,4], **Young-In Chi**[3,4], **Theresa M. Guerin**[1,2], **Eric J. Smart**[1,2], and **Jun Liu**[1,2,*]

[1]Department of Pediatrics, University of Kentucky, Lexington, KY, USA

[2]Kentucky Pediatric Research Institute, University of Kentucky, Lexington, KY, USA

[3]Department of Molecular and Cellular Biochemistry, University of Kentucky, Lexington, KY, USA

[4]Center for Structural Biology, University of Kentucky, Lexington, KY, USA

[5]Inserm U693, Faculté de Medécine ParisSud, Le Kremlin Bicetre, France

Summary

Adipose triglyceride lipase (ATGL) is the rate-limiting enzyme for triacylglycerol (TAG) hydrolysis in adipocytes. The precise mechanisms whereby ATGL is regulated remain uncertain. Here we demonstrate that a protein encoded by G_0/G_1 switch gene 2 (G0S2) is a selective regulator of ATGL. G0S2 is highly expressed in adipose tissue and differentiated adipocytes. When overexpressed in HeLa cells, G0S2 localizes to lipid droplets and prevents their degradation mediated by ATGL. Moreover, G0S2 specifically interacts with ATGL, requiring the hydrophobic domain of G0S2 and the patatin-like domain of ATGL. More importantly, interaction with G0S2 inhibits the TAG hydrolase activity of ATGL. Furthermore, knockdown of endogenous G0S2 accelerates basal and stimulated lipolysis in adipocytes, while overexpression of G0S2 diminishes the rate of lipolysis in both adipocytes and adipose tissue explants. Thus, G0S2 functions to attenuate ATGL action both *in vitro* and *in vivo*, underlying a novel mechanism for the regulation of TAG hydrolysis.

Introduction

During instances of heightened metabolic demand, TAG stores in lipid droplets of adipocytes undergo a hydrolytic process (lipolysis) to release FFAs and glycerol into the circulation for use by other organs (Duncan et al., 2007). The regulation of lipolysis in adipocytes has been well studied for nearly half a century, with most of the attention focused on hormone-sensitive lipase. In a well established model, the cAMP-dependent protein kinase (PKA) phosphorylates HSL and the lipid droplet coat protein perilipin A in response to β-adrenergic hormones. Consequently, HSL translocates from the cytoplasm onto lipid droplets, thereby mediating TAG hydrolysis (Egan et al., 1992; Sztalryd et al., 2003). However, the failure of HSL null mice to display an obese phenotype led to the discovery of an independent TAG hydrolase named adipose triglyceride lipase (ATGL) (Jenkins et al.,

*To whom correspondence should be addressed at: Department of Pediatrics, University of Kentucky, BBSRB B357, 741 South Limestone Street, Lexington, KY 40536-0509, Tel: (859) 257-4055, Fax: (859) 257-2120, jun.liu@uky.edu.

2004; Villena et al., 2004; Zimmermann et al., 2004). The complete lipolysis in adipocytes is delicately regulated and is now believed to be catalyzed sequentially by ATGL, HSL and monoacylglycerol (MAG) lipase (Raben and Baldassare, 2005; Watt and Steinberg, 2008; Zechner et al., 2009; Zimmermann et al., 2009).

ATGL is highly expressed in adipose tissue (Villena et al., 2004; Zimmermann et al., 2004). Its TAG hydrolase activity is dependent on a "patatin domain" common to plant acyl-transferases (Dessen et al., 1999; Rydel et al., 2003). Analysis using cultured cells demonstrated that ATGL was involved in basal and hormone-stimulated lipolysis in adipocytes (Bezaire et al., 2009; Kershaw et al., 2006; Zimmermann et al., 2004), and lipid droplet degradation in nonadipocyte cells (Smirnova et al., 2006). Most notably, ATGL null mice showed impaired lipolysis in adipocytes in response to β-adrenergic stimulation accompanied by an expanded adipose tissue mass and increased TAG deposition in most other tissues (Haemmerle et al., 2006). Exercise-induced lipolysis was also shown to be blunted in these mice (Huijsman et al., 2009). Conversely, adipose-specific overexpression of ATGL promoted lipolysis and attenuated diet-induced obesity in mice (Ahmadian et al., 2009). In humans, a subgroup of neutral lipid storage disease (NLSD) characterized by mild myopathy was reported to be caused by mutations in ATGL (Fischer et al., 2007). Although experiments using a specific HSL inhibitor and siRNA-mediated knockdown of ATGL suggested that in human fat HSL might be more important in mediating hormone-stimulated lipolysis (Langin et al., 2005; Ryden et al., 2007), a very recent study provided evidence that in human hMADS adipocytes ATGL acted independently of HSL and preceded its action in the sequential hydrolysis of TAG (Bezaire et al., 2009). Collectively, these studies have provided compelling evidence to establish ATGL as the key enzyme catalyzing adipocyte lipolysis.

In contrast to HSL, relatively little is known about the mechanisms whereby ATGL activity is regulated. Lass *et al* demonstrated that CGI-58 (Comparative Gene Identification 58) stimulates lipolysis and is an activator of ATGL but not HSL (Lass et al., 2006). Earlier studies identified mutations in the human CGI-58 gene as a cause for Chanarin-Dorfman syndrome (CDS), a rare form of NLSD characterized by ichthyosis (Lefevre et al., 2001). Interestingly, CGI-58 mutants associated with CDS failed to activate ATGL (Lass et al., 2006), implying that loss of ATGL activation may be involved in the pathogenesis of CDS. Moreover, ATGL was shown to interact physically with pigment epithelium-derived factor (PEDF) in liver (Chung et al., 2008; Notari et al., 2006). PEDF-deficient hepatocytes exhibited increased TAG accumulation, suggesting that PEDF also plays a positive role in regulating ATGL-mediated lipolysis. Furthermore, ATGL activity in adipocytes is known to be promoted by β-adrenergic stimulation (Haemmerle et al., 2006; Zimmermann et al., 2009). Although PKA does not appear to directly phosphorylate ATGL (Zimmermann et al., 2004), recent work by Miyoshi *et al*. demonstrated that phosphorylation of Ser517 in perilipin A was essential for activation of ATGL *in vivo* (Miyoshi et al., 2007).

Here we demonstrate that G_0/G_1 switch gene 2 (G0S2), a protein of previously unknown function, is a novel and negative regulator of ATGL. G0S2 was originally identified in blood mononuclear cells due to the association of its mRNA expression with re-entry of cells from G_0 into G_1 phase (Russell and Forsdyke, 1991). However, its role in cell cycle regulation has never been established. Zandbergen *et al*. later reported that the G0S2 mRNA level was highest in adipose tissue and was up-regulated during adipogenic differentiation of preadipocytes (Zandbergen et al., 2005). In this study, we performed functional analysis of G0S2 by using a variety of *in vitro* and cell-based approaches. Our results indicate that G0S2 binds directly to ATGL and is capable of attenuating ATGL-mediated lipolysis via inhibiting its TAG hydrolase activity.

Results

Expression pattern of G0S2 protein

To initiate functional studies, we raised antibodies against murine G0S2 (Fig. S1) and determined its expression pattern. Immunoblotting of various mouse tissues demonstrated an abundant expression of G0S2 in white and brown adipose tissues (WAT and BAT) and liver, and to a lesser degree in heart (Fig. 1A). The adipose-specific expression of G0S2 was corroborated in mouse white 3T3-L1 and brown T37i preadipocyte cell lines (Fig. 1B). In both cell types, G0S2 protein expression was first detected 4 days after adipogenic induction. The maximal level reached after 7 days when 3T3-L1 cells were fully differentiated, as judged by expression of an adipocyte marker aP2. In T37i cells, the G0S2 expression became robust after 5 days. UCP1, a brown adipocyte specific mitochondrial marker, appeared at the 7 day time point. These results indicate a differentiation dependent expression of G0S2 protein in adipocytes. In mouse WAT, amounts of G0S2 were significantly decreased in *db/db* mice compared with that of wild type mice (Fig. 1C). Chronic high-fat feeding of wild type mice also reduced the level of G0S2 in WAT, suggesting that G0S2 expression negatively correlates with the development of obesity.

Treatment with insulin profoundly increased G0S2 expression in both 3T3-L1 and T37i adipocytes (Fig. 1D). Conversely, prolonged treatment with β-adrenergic agonist isoproterenol or another lipolysis inducing hormone TNFα drastically decreased G0S2 level in both cell types. Moreover, no effects were observed when adipocytes were treated with GW501516 (a PPARδ ligand) or T3 (thyroid hormone). Rosiglitazone, however, significantly enhanced G0S2 expression in both cell types, confirming that G0S2 is a PPARγ downstream target (Zandbergen et al., 2005).

G0S2 prevents lipid droplet turnover mediated by ATGL

To obtain further insight into the potential function of G0S2, we expressed G0S2 in HeLa cells and determined its subcellular localization by immunofluorescence staining. As shown in Fig. 2A, G0S2 displayed a pattern of small rings that scattered throughout the cytoplasm. Using BODIPY 493/503, a nonpolar probe selective for neural lipids such as TAG, we identified that these ring-like structures surrounded the central cores of lipid droplets. Since lipid droplets undergo constant synthesis and turnover (Martin and Parton, 2006), we next examined the potential involvement of G0S2 in regulating lipid droplet stability. HeLa cells transiently expressing G0S2 were treated with oleic acid for 3 hrs to promote lipid droplet formation (Fig. 2B). Lipid droplets in cells expressing G0S2 were significantly larger and more numerous than those in the neighboring untransfected cells (Fig. 2B, upper panel). Overloading the cells with oleic acid for 24 hrs resulted in accumulation of large lipid droplets in both transfected and untransfected cells with no obvious difference in size and number (Fig. 2B, middle panel). However, after 24 hrs of oleic acid treatment followed by nutrient starvation for 4 hrs, lipid droplets in untransfected cells underwent pronounced degradation while overexpression of G0S2 was able to prevent such turnover (Fig. 2B, lower panel). For the three experimental conditions employed, the average diameter of lipid droplets in untransfected cells vs. G0S2-transfected cells was 0.45 μm vs. 0.89 μm, 1.13 μm vs. 1.22 μm, and 0.34 μm vs. 0.99 μm, respectively (Fig. 2C).

Since ATGL plays a key role in lipid droplet degradation in HeLa cells (Smirnova et al., 2006), we tested whether G0S2 would neutralize this effect of ATGL action. Upon oleic acid loading, HeLa cells transfected with ATGL alone showed a marked reduction in both size and number of lipid droplets compared with the adjacent untransfected controls (Fig. 3A, upper panel). Interestingly, coexpression of G0S2 tagged at the C-terminus with a FLAG epitope (G0S2-FLAG) was able to reverse this effect of ATGL overexpression (Fig.

3A, middle panel). Consequently, G0S2-FLAG and ATGL were found to be co-localized at the surface of lipid droplets (Fig. 3A, lower panel). To further assess whether G0S2 and ATGL, singly or in combination, affect intracellular TAG accumulation, we generated HeLa cells stably expressing untagged G0S2 and then employed siRNA to knockdown ATGL in these cells. The knockdown was equally effective at reducing endogenous ATGL in both G0S2-expressing and non-expressing cells (Fig. 3B). Less than 5% of ATGL was present in cells transfected with a pool of siRNAs directed against ATGL compared with cells transfected with a mismatched control siRNA. The TAG content in G0S2-expressing cells was profoundly increased upon oleic acid treatment compared with that in non-expressing control cells (Fig. 3C). Knockdown of ATGL promoted TAG accumulation in control cells, presumably due to decreased TAG hydrolysis. Strikingly, the effects of reduced ATGL expression and G0S2 overexpression are not additive, since ATGL knockdown failed to further increase the TAG content in G0S2-expressing cells (Fig. 3C). Taken together, these results suggest that G0S2 expression may stabilize lipid droplets and promote TAG accumulation via inhibiting ATGL-catalyzed lipolysis.

G0S2 inhibits TAG hydrolase activity of ATGL

Murine G0S2 is a 103-amino acid protein with a central putative hydrophobic domain (residues 27–42) (Zandbergen et al., 2005). ATGL, on the other hand, belongs to a family of lipases containing a patatin domain essential for their hydrolase activity (Watt and Steinberg, 2008; Zimmermann et al., 2009). The C-terminal region of ATGL contains a putative lipid-binding domain that is highly hydrophobic (Fischer et al., 2007; Kobayashi et al., 2008; Schweiger et al., 2008) (Fig. 4A). To determine whether G0S2 could regulate TAG hydrolase activity of ATGL, we transfected ATGL in G0S2-expressing or non-expressing HeLa cells (Fig. 4B). In assays with lysates of non-expressing control cells, transfection of ATGL resulted in an over 4-fold increase in the TAG hydrolase activity when compared to transfection of vector alone. By contrast, overexpression of ATGL in G0S2-expressing cells failed to significantly enhance the lipase activity. G0S2 also significantly reduced the activity of ATGLΔHD, a mutant that lacks the putative lipid-binding hydrophobic domain (Fig. 4B). As a control, expression of HSL increased lipase activity by ~10-fold independently of G0S2 expression (Fig. S2). Therefore, the presence of G0S2 substantially inhibits the enzymatic activity of ATGL but not that of HSL.

Since ATGL is activated by CGI-58 (Lass et al., 2006), we investigated whether G0S2 could affect the TAG hydrolase activity of ATGL in the presence of CGI-58. To this end, ATGL, CGI-58 and G0S2 were expressed singly in HeLa cells and then the TAG hydrolase activity was measured in combined cell extracts (Fig. 4C). The addition of CGI-58-containing extracts to ATGL-containing extracts caused a ~4-fold increase in the TAG hydrolase activity. However, the further addition of G0S2-containing extracts to the mixture considerably eliminated this activating effect of CGI-58, indicating that G0S2 is capable of inhibiting ATGL even in the presence of CGI-58. Similar results were obtained by adding recombinant G0S2 protein expressed and purified from *E. coli* to ATGL and CGI-58 produced from an *in vitro* transcription/translation system. As shown in Fig. 4D, purified G0S2 dose-dependently inhibited the TAG hydrolase activity of ATGL both in the absence and in the presence of CGI-58. Moreover, varying amounts of purified G0S2 were added to mouse WAT and BAT extracts, with the highest concentration decreasing their total TAG hydrolase activity by 32% and 38%, respectively (Fig. 4E). The differences are significant considering that although ATGL is the main TAG hydrolase *in vivo*, a large portion of the total *in vitro* activity towards TAG substrate is accounted for by HSL and therefore may not be affected by G0S2.

G0S2 directly interacts with ATGL

To determine if G0S2 physically interacts with ATGL, we transiently expressed ATGL and G0S2-FLAG in HeLa cells and evaluated their interaction by co-immunoprecipitation assays (Fig. 5A). As revealed by immunoblotting of total proteins from cell lysates, comparable levels of ATGL were expressed with or without G0S2-FLAG. Anti-FLAG immunoprecipitation demonstrated a specific association of ATGL with precipitated G0S2-FLAG. To identify the structural determinants required for the G0S2-ATGL interaction, we generated several deletion mutants of G0S2 and ATGL (Fig. 4A). While $G0S2_{1–73}$ contains the N-terminal 73 amino acids including an intact hydrophobic domain, G0S2ΔHD is an internal deletion mutant lacking the hydrophobic domain. Meanwhile, ATGLΔPT and ATGLΔHD are two internal deletion mutants that lack the patatin domain (residues 10–178) and the hydrophobic domain (residues 259–337), respectively. As shown in Fig. 5A, G0S2-FLAG co-immunoprecipitated with both wild type ATGL and ATGLΔHD mutant, while ATGLΔPT mutant exhibited no interaction with G0S2-FLAG. In a separate experiment, $G0S2_{1–73}$-FLAG was found to interact with ATGL with the same affinity as the full-length G0S2-FLAG. However, G0S2ΔHD-FLAG showed no binding to ATGL (Fig. 5B). Therefore, the hydrophobic domain in G0S2 and the patatin domain of ATGL are needed for mediating the specific association.

To determine whether interaction occurs between the endogenous proteins, ATGL was immunoprecipitated from 3T3-L1 adipocyte lysates with anti-ATGL antibodies. As controls, immunoprecipitation was performed using nonspecific or anti-HSL antibodies as well as using ATGL antibodies in the presence of an ATGL blocking peptide. As shown in Fig. 5C, endogenous ATGL and HSL were efficiently pulled down by respective antibodies. G0S2 was specifically coimmunoprecipitated with ATGL but not with HSL. The blocking peptide was able to abolish both immunoprecipitation of ATGL and coimmunoprecipitation of G0S2 by ATGL antibodies, demonstrating the specificity of their association. The complex formation appears to be stable since pretreatment of cells with either isoproterenol or insulin conferred no significant impact on the G0S2-ATGL coimmunoprecipitation (Fig. 5C).

To exclude the possibility that the complex formation is bridged by a third protein in cells, we assayed the interaction between G0S2 and ATGL proteins produced by *in vitro* transcription/translation system (Fig. 5D). As expected, ATGL was co-immunoprecipitated with G0S2-FLAG when they were present in the same reaction, demonstrating a direct association *in vitro*. The association with ATGL required the hydrophobic domain of G0S2, since ATGL did not coprecipitate with an internal deletion mutant of G0S2 (G0S2ΔHD-FLAG) (Fig. 5D). In addition, we analyzed the TAG hydrolase activity in reaction mixtures containing ATGL with wild type G0S2-FLAG or G0S2ΔHD-FLAG (Fig. 5E). G0S2-FLAG decreased the TAG hydrolase activity in ATGL-containing mixture by ~70%, while G0S2ΔHD-FLAG had no significant effect, indicating that direct interaction is necessary for efficient inhibition of ATGL by G0S2.

Lipid droplet localization of G0S2 in adipocytes depends on interaction with ATGL

ATGL activity *in vivo* is determined by its lipid droplet localization (Fischer et al., 2007; Kobayashi et al., 2008; Schweiger et al., 2008). To analyze the relative localization of endogenous ATGL and G0S2, we performed lipid droplet fractionation experiments using 3T3-L1 adipocytes (Fig. 6A). In basal state, only low levels of HSL, ATGL and G0S2 were detected in the association with lipid droplets. Insulin treatment mildly increased the amounts of ATGL and G0S2 but not HSL in the lipid droplet fraction. As expected, stimulation of lipolysis with isoproterenol promoted translocation of HSL to lipid droplet fraction where upward shift of perilipin was also observed due to PKA phosphorylation. Interestingly, isoproterenol also caused a marked movement of both ATGL and G0S2 to

lipid droplets (Fig. 6A). A time course experiment showed a rapid and sustained accumulation of ATGL and G0S2 in lipid droplets over the course of 10–120 min post stimulation (Fig. S3). Lipid droplet translocation of ATGL and G0S2 was independently confirmed by immunofluorescence microscopy as isoproterenol caused redistribution of ATGL and G0S2 staining from cytoplasm to rim-like structures surrounding lipid droplets (Fig. 6B). To determine whether G0S2 moves onto lipid droplets in a complex with ATGL, we tested the effect of ATGL knockdown on the lipid droplets translocation of G0S2. As revealed immunoblotting in Fig. 6C, an approximately 90% knockdown efficiency was achieved by the combined usage of a pool of siRNAs against murine ATGL in comparison to mismatched controls. Interestingly, knockdown of ATGL expression reduced overall level of G0S2 protein while had no effect on the expression of HSL and perilipin. More importantly, G0S2 was absent in the lipid droplet fraction isolated from isoproterenol-treated cells transfected with ATGL siRNA (Fig. 6C), suggesting that the lipid droplet localization of G0S2 may indeed depend on its interaction with ATGL.

G0S2 attenuates lipolysis in adipocytes

The findings that G0S2 interacts with and inhibits ATGL prompted us to investigate the potential role of G0S2 in adipocyte lipolysis. To this end, we reduced the G0S2 level in 3T3-L1 adipocytes by siRNA-mediated knockdown. Compared with mismatch control siRNA, the siRNA directed against G0S2 was effective at inhibiting G0S2 expression in 3T3-L1 adipocytes (Fig. 7A). Importantly, lipolysis in 3T3-L1 cells was significantly enhanced by G0S2 knockdown in a time-dependent manner. After a 2-hr incubation period, basal and isoproterenol-stimulated FFA release was increased by 103% and 75%, respectively (Fig. 7A). The effect of G0S2 knockdown on glycerol release followed the same trend though it was less prominent (Fig. 7A).

To corroborate our knockdown results, we performed gain of function studies by infecting adipocytes with an adenovirus encoding murine G0S2 (Ad-G0S2). Two different dosages of Ad-G0S2 and a null virus were employed, with the higher dose of Ad-G0S2 achieving a ~4-fold increase in G0S2 expression in 3T3-L1 adipocytes (Fig. 7B). Infection of 3T3-L1 cells with Ad-G0S2 at this higher dosage significantly reduced basal and stimulated-lipolysis when compared to infection with the null virus. In addition, infection of WAT explants with Ad-G0S2 virus inhibited isoproterenol -stimulated FFA release by ~40% (Fig. 7C). However, ectopic expression of G0S2 in WAT explants only had a mild effect on basal FFA release. Nonetheless, these results collectively demonstrate a critical role of G0S2 in the control of adipose lipolysis.

Discussion

As a closely controlled process essential for survival, lipolysis in adipocytes has been well studied for several decades. The discovery of ATGL as the key enzyme in adipocyte lipolysis is relatively recent (Zimmermann et al., 2009), and how ATGL activity is regulated is mostly unknown. The present study provides compelling evidence that G0S2 is an important negative regulator of ATGL-mediated lipolysis. Like ATGL (Fig. 1A & 1B) (Villena et al., 2004; Zimmermann et al., 2004), G0S2 protein is highly expressed in adipose tissue, and its expression was induced during adipocyte differentiation. Biochemically, G0S2 binds directly to ATGL and is capable of inhibiting its TAG hydrolase activity. Functionally, overexpression of G0S2 prevents ATGL-mediated lipid droplet degradation in HeLa cells as well as basal and stimulated lipolysis in cultured adipocytes and fat explants. Knockdown of endogenous G0S2, on the other hand, enhances adipocyte lipolysis under the same conditions.

G0S2 is a small basic protein with 78% identity between mouse and human isoforms. It has no homologs in lower organisms such as *Caenorhabditis elegans* and *Drosophila*. Our deletion mutagenesis experiments showed that the putative hydrophobic domain of G0S2 and the catalytic patatin-like domain of ATGL were responsible for mediating their specific interaction. Moreover, knockdown of ATGL decreased the overall content of G0S2 in adipocytes, indicating that intracellular stability of G0S2 may be enhanced by its interaction with ATGL. Although detailed structural studies are needed to delineate the possible mechanisms for inhibition of ATGL lipase activity by G0S2, we speculate that G0S2 binding may directly affect the substrate (TAG) accessibility or simply alter the overall conformation of ATGL. Aside from being a TAG hydrolase, ATGL possess activity as an acyl-CoA-independent transacylase, utilizing acylglycerols such as monoolein or diolein as acyl donors/acceptors in the production of TAG (Jenkins et al., 2004). Therefore, it is also possible that the G0S2 binding can decrease the net fatty acid release in a futile cycle by promoting ATGL-mediated transacylation of DAG and MAG back to TAG. Furthermore, we found that G0S2 was capable of dose-dependently inhibiting ATGL even in the presence of the co-activator CGI-58, though CGI-58 rendered ATGL less sensitive to G0S2 inhibition. Since CGI-58 binds to the same N-terminal region of ATGL (Lass et al., 2006; Schweiger et al., 2008), it would be interesting to determine whether CGI-58 and G0S2 directly compete with each other in the control of ATGL lipase activity.

The expression of G0S2 is subject to hormonal and nutritional regulation. Previous studies have shown that G0S2 mRNA level is upregulated by insulin in skeletal muscle (Parikh et al., 2007), by glucose in liver (Ma et al., 2006), and by PPARγ agonists in adipocytes (Zandbergen et al., 2005), indicating its role in energy metabolism. We found that G0S2 in adipocytes was reciprocally regulated by insulin and lipolytic simulators. In contrast to reduced expression of ATGL (Fig. 1D) (Kershaw et al., 2006), prolonged insulin treatment significantly upregulated G0S2 protein expression in adipocytes. Chronic treatment with isoproterenol and TNFα, on the other hand, drastically downregulated the level of G0S2. The fact that the expression of G0S2 as a lipolytic inhibitor can alter according to anabolic vs. catabolic conditions implicates a potential mechanism to switch the balance between TAG mobilization and storage. In cases of caloric surplus, for example, an insulin-induced increase in the ratio between G0S2 and ATGL levels may lead to lower lipolytic capacity and thus serve to facilitate the flow of fatty acid into TAG in WAT. During chronic exposure to starvation, catecholamines can turn off the expression of G0S2 as a way to sustain lipolysis in adipocytes.

By both lipid droplet fractionation and immunofluorescence staining, we demonstrated that isoproterenol treatment promoted rapid and dramatic translocation of ATGL from cytoplasm to the surface of lipid droplets. The observation that ATGL underwent HSL-like translocation to lipid droplets in response to lipolytic stimulation is potentially very important. The ATGL enzyme action, which is dependent on its lipid droplet localization, is known to be sensitive to β-adrenergic stimulation in adipocytes (Zimmermann et al., 2009). However, unlike HSL, ATGL activity does not appear to be regulated directly by PKA phosphorylation (Zimmermann et al., 2004). Two previous studies demonstrated either no or a modest translocation of ATGL to lipid droplets in lipolytically stimulated cells (Granneman et al., 2007; Zimmermann et al., 2004). This discrepancy from our findings may be due to the fact that the previous experiments employed transient overexpression of epitope-tagged proteins, whereas our observations were made on endogenous ATGL. Similarly, Bezaire *et al.* showed that forskolin stimulated translocation of both HSL and ATGL to lipid droplets in human hMADs adipocytes (Bezaire et al., 2009). Together these findings implicate a potential mechanism for the activation of ATGL *in vivo* in response to β-adrenergic stimulation. Interestingly, Miyoshi et al. showed that ATGL action in adipocytes was controlled by PKA phosphorylation of Serine 517 of perilipin A (Miyoshi et

al., 2007). Therefore, it would be tempting to examine whether this phosphorylation event plays any role in the redistribution of ATGL to lipid droplets. Also worth mentioning is a mild accumulation of ATGL and G0S2 in lipid droplets induced by insulin treatment of adipocytes. The precise signaling mechanisms and functional relevance of this observation are currently unknown. We speculate that ATGL, some of which is in the form of ATGL/G0S2 complex, may move onto lipid droplets as a feedback response to lipolytic inhibition or/and lipogenic stimulation elicited by insulin. Prolonged insulin treatment is able to downregulate ATGL expression, thereby reversing this process.

As revealed by coimmunoprecipitation, the interaction between ATGL and G0S2 was not subject to regulation by isoproterenol. Based upon this observation, we speculate that at least a small fraction of ATGL is constantly in complex with G0S2, both in the basal state and during the acute stage of lipolytic stimulation. Although G0S2-bound ATGL is not fully active, it is conceivable that not all ATGL is in association with G0S2 and isoproterenol-stimulated translocation of this free fraction would still allow profound activation of lipolysis (Fig. 8). Two lines of evidence we obtained are supportive of this hypothesis. Firstly, G0S2 underwent similar translocation from cytoplasm to lipid droplets upon isoproterenol treatment. This redistribution was abolished by the knockdown of ATGL, indicating that G0S2 is piggybacked onto lipid droplets by ATGL. The result is consistent with our other finding that the G0S2 binding does not involve the lipid-binding hydrophobic domain of ATGL, allowing simultaneous association of ATGL to G0S2 and lipid droplets. Secondly, through knockdown and overexpression of G0S2 thereby altering the ratio between free ATGL and G0S2-bound ATGL, we were able to accordingly alter the lipolytic rates in adipocytes.

G0S2 was previously shown to be localized to the endoplasmic reticulum (ER) when expressed in HEK293 cells as well as 3T3-L1 preadipocytes (Zandbergen et al., 2005). ATGL, on the other hand, was found to be tightly associated with membranes when not localized to lipid droplets in HeLa cells (Soni et al., 2009). Therefore, it is possible that in adipocytes both G0S2 and ATGL also occur in association with an ER-related membrane compartment, from which they are recruited onto lipid droplets upon adrenergic stimulation. In this regard, it would be interesting to determine whether coatmer protein I (COPI) complex, the membrane trafficking machinery responsible for delivering ATGL to lipid droplets in non-adipocytes (Beller et al., 2008; Soni et al., 2009), is also employed for lipid droplet recruitment of ATGL and G0S2 in adipocytes.

Lastly, we found that G0S2 expression was significantly reduced in WAT of *db/db* mice and high fat-fed wild type mice. Since obesity is associated with insulin resistance in peripheral tissues, we speculate that impaired insulin sensitivity of adipocytes may lead to the decreased expression of G0S2. It is also possible that increased production of TNFα by WAT during obesity plays a role in downregulating G0S2 expression, considering that G0S2 level was diminished in adipocytes upon TNFα treatment (Fig. 1D). Moreover, elevated basal lipolytic capacity of adipocytes is known to contribute to increased plasma FFA levels in human obesity (Boden and Shulman, 2002; Guilherme et al., 2008; Watt and Steinberg, 2007), and thus may represent an important risk factor for the development of insulin resistance and type 2 diabetes. Accordingly, further studies will be undertaken to investigate whether expression of G0S2 is also decreased in obese human. If so, it would be important to determine whether a reduced level of G0S2 contributes to the elevated lipolysis associated with obesity.

Experimental Procedures

Production and purification of bacterially expressed G0S2

The full-length mouse G0S2 cDNA was subcloned by standard PCR into pET41a MBP vector (Lu et al., 2008) to produce the protein fused with MBP at the N-terminal end with the TEV cleavage site. For tag-free protein purification, G0S2 was overexpressed in Escherichia coli BL21-Gold (Novagen) with induction of 0.5 mM IPTG at an A600 of 0.8–1.0 at 37 °C and harvested after culturing for an additional 4–6 h. The cells were lysed by sonication, and the expressed MBP-fusion proteins were isolated in the presence of 0.6 M NaCl to prevent nonspecific binding to bacterial DNA.G0S2 was released by TEV digestion from amylase magnetic beads (New England Biolabs) after overnight incubation at 4 °C and further purified by ion exchange chromatography (Mono-S FPLC). The purified protein was estimated to be at least 98% pure as judged by staining with Coomassie Brilliant Blue on an 8–25% gradient SDS-polyacrylamide gel. Fractions were pooled; concentrations were measured by UV absorption and dialyzed into PBS buffer containing 0.25 M sucrose, 1 mM EDTA and 1 mM DTT.

siRNA-mediated knockdown

The following double stranded stealth siRNA oligonucleotides (Invitrogen) were used: set 1 for mouse G0S2, sense 5’ CAUGCUGUUUCAAGGUGCCACCGAA 3’, antisense 5’ UUCGGUGGCACCUUGAAACAGCAUG 3’; set 2 for mouse G0S2, sense 5’CACCGAAUCCAGAACUGACCCUACA3’, antisense 5’UGUAGGGUCAGUUCUGGAUUCGGUG3’; human ATGL, set of 3 validated siRNA oligonucleotides (Cat# 1299003); mouse ATGL, set of 3 validated oligonucleotides (Cat# 1320003). Control oligonucleotides with comparable GC content were also from Invitrogen.

For ATGL knockdown in HeLa cells, total 100 pmole of mixed oligonucleotides, 33 pmole of each of the three sets, were transfected into HeLa cells plated in 6-well dishes using Lipofectamine 2000. For ATGL and G0S2 knockdown in 3T3-L1 and T37i adipocytes, 4 nmole of mixed oligonucleotides, 2 nmole of each of the three sets, were delivered into cells via electroporation using BioRad Gene Pulser II at 950 μF and 160V as described previously (Chen et al., 2007). After 3 days of incubation, cells were processed for designated assays.

Adenoviral infection of adipocytes and adipose tissue explants

Recombinant adenovirus containing murine G0S2 cDNA under the control of a CMV promoter (Ad-G0S2) was custom generated by Vector Biolabs. A CMV null virus (Adnull) was also obtained for use in control experiments. Infection of differentiated adipocytes and adipose tissue explants was performed by using a previously published method (Greenberg et al., 2003) with minor modifications. For infection of 3T3-L1 and T37i adipocytes, Ad-G0S2 or Ad-null were diluted to two concentrations (10^7 and 10^8 pfu/ml) in DMEM, 2% FBS, and 5.0 μg/ml polybrene and preincubated for 45 min at room temperature. Adipocytes in 6-well dishes were washed once with PBS, and 1.2 ml of preincubated virus mix was added to each well. Cells were centrifuged at 800 × g for 1 h at room temperature followed by incubation at 37°C. 1.0 ml/well of fresh growth medium was added after 4 h, and cells were incubated for 48–72 h before use. Adipocytes in 6-well dishes were washed once with PBS, and 1.2 ml of preincubated virus mix was added to each well. Cells were centrifuged at 800 × g for 1 h at room temperature followed by incubation at 37°C. 1.0 ml/well of fresh growth medium was added after 4 h, and cells were incubated for 72 h before use. For infection of adipose tissue explants, gonadal fat pads (~25 mg) freshly isolated from 20-week-old C57BL6 female mice were washed with PBS and then incubated in a microcentrifuge tube containing 150 μl of virus mix (7×10^8 pfu/ml) for 45 min at room temperature. Following centrifugation at 800 × g for 1 h at room temperature, explants along

with virus mix were transferred to a 24-well dish and incubated at 37°C. 0.5 ml/well of fresh growth medium was added after 4 h, and explants were incubated for 48 h before use.

Lipid droplet fractionation

Lipid droplets were isolated from 3T3-L1 adipocytes as describe previously (Brasaemle and Wolins, 2006). Briefly, cells were collected in ice-cold PBS followed by centrifugation for 10 min at 1000 × g, 4 °C. Cell pellets were resuspended in HLM buffer (20 mM Tris•Cl, pH 7.4, 1 mM, 0.5 mM EDTA, 10 mM sodium fluoride and protease inhibitors) and homogenized by 10 gentle strokes with a hand-driven pestle. The homogenates were centrifuged for 10 min at 1,000 × g, 4 °C. The supernatant was collected and the floating lipid layer was transferred into a separate ultracentrifugation tube. 1/3 volume of ice-cold HLM containing 60% sucrose (final 20% sucrose) was added, and lipid droplets were mixed thoroughly by gentle pipetting. The mixture was then overloaded sequentially with HLM containing 5% sucrose and HLM containing no sucrose. After centrifugation for 30 min at 28,000 × g, 4 °C, the floating lipid droplet fraction was collected by using a Beckman tube slicer. Equal volume of 10% SDS was added and proteins associated with lipid droplets were solubilized by incubation for 2 h at 37°C in a sonicating water bath.

Assay for TAG hydrolase activity

For assays with HeLa cell extracts, cells in 10-cm dishes were washed twice in ice-cold PBS and then disrupted on ice by passing 10 times through a 22G needle in 0.5 ml of cell extraction buffer (0.25 M sucrose, 1 mM EDTA, 1 mM DTT and protease inhibitors (1 mini tablet per 7 ml of volume)). For assays with WAT and BAT, epididymal and interscapular fat pads were homogenized in cell extraction buffer by a drill press as describe above. The cell and tissue extracts were clarified by centrifugation at 1,000 × g for 15 min. The TAG hydrolase activity against ^{3}H-labeled triolein was measured as described previously (Lass et al., 2006; Zimmermann et al., 2004) by mixing 0.1 ml of extracts with 0.1 ml of substrate solution. For assays using *in vitro* transcription/translation products, a total of 35 μl of reaction mixture was pre-diluted with 65 μl of cell extraction buffer. The resulting 0.1 ml of reaction mixture was then combined with 0.1 ml of substrate solution in the TAG hydrolase activity measurement.

Lipolysis assay and measurement of intracellular TAG content

Lipolysis was measured as the rate of glycerol and free fatty acid release. Briefly, adipocytes or gonadal WAT explants in 12-well dishes were incubated in 1 ml of assay buffer in the presence or absence of 1 μM isoproterenol. Aliquots of assay buffer were collected over a 30 min-2h period. The amounts of glycerol and FFAs released were determined by using a lipolysis assay kit (Zenbio) according to the manufacturer's instructions. Lysates were then prepared from the remaining cells, and protein concentrations in the lysates were used to normalize the lipolytic signals.

Triglyceride accumulation was measured using a triglyceride assay kit (Zenbio). Briefly, at the indicated time after oleic acid treatment, HeLa cells were washed and lysed in provided lysis buffer. Then the triglyceride assay reagents were added according to the manufacturer's instructions. The optical density of the solution was measured at 540 nm using a spectrophotometer plate reader. TAG concentration was calculated from a standard curve for each assay, and data is normalized to total cellular protein.

Supplementary Material

Refer to Web version on PubMed Central for supplementary material.

Acknowledgments

We thank Drs. Carole Sztalryd, Matthew J. Brady, Xiaowei Chen, Alan Cheng and William V. Everson for reviewing the manuscript and helpful discussions. We also thank Dr. Say Viengchareun for excellent technical advice. The work was supported by a NIH grant DK 078742 and a Center of Biomedical Research Excellence pilot grant from the University of Kentucky (5P20 RR0202171) to J.L., and NIH grants RR015592 and DK077632 to E.J.S.

References

Ahmadian M, Duncan RE, Varady KA, Frasson D, Hellerstein MK, Birkenfeld AL, Samuel VT, Shulman GI, Wang Y, Kang C, Sul HS. Adipose overexpression of desnutrin promotes fatty acid use and attenuates diet-induced obesity. Diabetes. 2009; 58:855–866. [PubMed: 19136649]

Beller M, Sztalryd C, Southall N, Bell M, Jackle H, Auld DS, Oliver B. COPI complex is a regulator of lipid homeostasis. PLoS Biol. 2008; 6:e292. [PubMed: 19067489]

Bezaire V, Mairal A, Ribet C, Lefort C, Girousse A, Jocken J, Laurencikiene J, Anesia R, Rodriguez AM, Ryden M, Stenson BM, Dani C, Ailhaud G, Arner P, Langin D. Contribution of adipose triglyceride lipase and hormone-sensitive lipase to lipolysis in hMADS adipocytes. J Biol Chem. 2009; 284:18282–18291. [PubMed: 19433586]

Boden G, Shulman GI. Free fatty acids in obesity and type 2 diabetes: defining their role in the development of insulin resistance and beta-cell dysfunction. Eur J Clin Invest. 2002; 32(Suppl 3): 14–23. [PubMed: 12028371]

Brasaemle DL, Wolins NE. Chapter 3 Isolation of lipid droplets from cells by density gradient centrifugation. Curr Protoc Cell Biol. 2006 Unit 3 15.

Chen XW, Leto D, Chiang SH, Wang Q, Saltiel AR. Activation of RalA is required for insulin-stimulated Glut4 trafficking to the plasma membrane via the exocyst and the motor protein Myo1c. Dev Cell. 2007; 13:391–404. [PubMed: 17765682]

Chung C, Doll JA, Gattu AK, Shugrue C, Cornwell M, Fitchev P, Crawford SE. Anti-angiogenic pigment epithelium-derived factor regulates hepatocyte triglyceride content through adipose triglyceride lipase (ATGL). J Hepatol. 2008; 48:471–478. [PubMed: 18191271]

Dessen A, Tang J, Schmidt H, Stahl M, Clark JD, Seehra J, Somers WS. Crystal structure of human cytosolic phospholipase A2 reveals a novel topology and catalytic mechanism. Cell. 1999; 97:349–360. [PubMed: 10319815]

Duncan RE, Ahmadian M, Jaworski K, Sarkadi-Nagy E, Sul HS. Regulation of lipolysis in adipocytes. Annu Rev Nutr. 2007; 27:79–101. [PubMed: 17313320]

Egan JJ, Greenberg AS, Chang MK, Wek SA, Moos MC Jr, Londos C. Mechanism of hormone-stimulated lipolysis in adipocytes: translocation of hormone-sensitive lipase to the lipid storage droplet. Proc Natl Acad Sci U S A. 1992; 89:8537–8541. [PubMed: 1528859]

Fischer J, Lefevre C, Morava E, Mussini JM, Laforet P, Negre-Salvayre A, Lathrop M, Salvayre R. The gene encoding adipose triglyceride lipase (PNPLA2) is mutated in neutral lipid storage disease with myopathy. Nat Genet. 2007; 39:28–30. [PubMed: 17187067]

Granneman JG, Moore HP, Granneman RL, Greenberg AS, Obin MS, Zhu Z. Analysis of lipolytic protein trafficking and interactions in adipocytes. J Biol Chem. 2007; 282:5726–5735. [PubMed: 17189257]

Greenberg CC, Meredith KN, Yan L, Brady MJ. Protein targeting to glycogen overexpression results in the specific enhancement of glycogen storage in 3T3-L1 adipocytes. J Biol Chem. 2003; 278:30835–30842. [PubMed: 12805359]

Guilherme A, Virbasius JV, Puri V, Czech MP. Adipocyte dysfunctions linking obesity to insulin resistance and type 2 diabetes. Nat Rev Mol Cell Biol. 2008; 9:367–377. [PubMed: 18401346]

Haemmerle G, Lass A, Zimmermann R, Gorkiewicz G, Meyer C, Rozman J, Heldmaier G, Maier R, Theussl C, Eder S, Kratky D, Wagner EF, Klingenspor M, Hoefler G, Zechner R. Defective lipolysis and altered energy metabolism in mice lacking adipose triglyceride lipase. Science. 2006; 312:734–737. [PubMed: 16675698]

Huijsman E, van de Par C, Economou C, van der Poel C, Lynch GS, Schoiswohl G, Haemmerle G, Zechner R, Watt MJ. Adipose triacylglycerol lipase deletion alters whole body energy metabolism

and impairs exercise performance in mice. Am J Physiol Endocrinol Metab. 2009; 297:E505–E513. [PubMed: 19491295]

Jenkins CM, Mancuso DJ, Yan W, Sims HF, Gibson B, Gross RW. Identification, cloning, expression, and purification of three novel human calcium-independent phospholipase A2 family members possessing triacylglycerol lipase and acylglycerol transacylase activities. J Biol Chem. 2004; 279:48968–48975. [PubMed: 15364929]

Kershaw EE, Hamm JK, Verhagen LA, Peroni O, Katic M, Flier JS. Adipose triglyceride lipase: function, regulation by insulin, and comparison with adiponutrin. Diabetes. 2006; 55:148–157. [PubMed: 16380488]

Kobayashi K, Inoguchi T, Maeda Y, Nakashima N, Kuwano A, Eto E, Ueno N, Sasaki S, Sawada F, Fujii M, Matoba Y, Sumiyoshi S, Kawate H, Takayanagi R. The lack of the C-terminal domain of adipose triglyceride lipase causes neutral lipid storage disease through impaired interactions with lipid droplets. J Clin Endocrinol Metab. 2008; 93:2877–2884. [PubMed: 18445677]

Langin D, Dicker A, Tavernier G, Hoffstedt J, Mairal A, Ryden M, Arner E, Sicard A, Jenkins CM, Viguerie N, van Harmelen V, Gross RW, Holm C, Arner P. Adipocyte lipases and defect of lipolysis in human obesity. Diabetes. 2005; 54:3190–3197. [PubMed: 16249444]

Lass A, Zimmermann R, Haemmerle G, Riederer M, Schoiswohl G, Schweiger M, Kienesberger P, Strauss JG, Gorkiewicz G, Zechner R. Adipose triglyceride lipase-mediated lipolysis of cellular fat stores is activated by CGI-58 and defective in Chanarin-Dorfman Syndrome. Cell Metab. 2006; 3:309–319. [PubMed: 16679289]

Lefevre C, Jobard F, Caux F, Bouadjar B, Karaduman A, Heilig R, Lakhdar H, Wollenberg A, Verret JL, Weissenbach J, Ozguc M, Lathrop M, Prud'homme JF, Fischer J. Mutations in CGI-58, the gene encoding a new protein of the esterase/lipase/thioesterase subfamily, in Chanarin-Dorfman syndrome. Am J Hum Genet. 2001; 69:1002–1012. [PubMed: 11590543]

Lu P, Rha GB, Melikishvili M, Wu G, Adkins BC, Fried MG, Chi YI. Structural basis of natural promoter recognition by a unique nuclear receptor, HNF4alpha. Diabetes gene product. J Biol Chem. 2008; 283:33685–33697. [PubMed: 18829458]

Ma L, Robinson LN, Towle HC. ChREBP*Mlx is the principal mediator of glucose-induced gene expression in the liver. J Biol Chem. 2006; 281:28721–28730. [PubMed: 16885160]

Martin S, Parton RG. Lipid droplets: a unified view of a dynamic organelle. Nat Rev Mol Cell Biol. 2006; 7:373–378. [PubMed: 16550215]

Miyoshi H, Perfield JW 2nd, Souza SC, Shen WJ, Zhang HH, Stancheva ZS, Kraemer FB, Obin MS, Greenberg AS. Control of adipose triglyceride lipase action by serine 517 of perilipin A globally regulates protein kinase A-stimulated lipolysis in adipocytes. J Biol Chem. 2007; 282:996–1002. [PubMed: 17114792]

Notari L, Baladron V, Aroca-Aguilar JD, Balko N, Heredia R, Meyer C, Notario PM, Saravanamuthu S, Nueda ML, Sanchez-Sanchez F, Escribano J, Laborda J, Becerra SP. Identification of a lipase-linked cell membrane receptor for pigment epithelium-derived factor. J Biol Chem. 2006; 281:38022–38037. [PubMed: 17032652]

Parikh H, Carlsson E, Chutkow WA, Johansson LE, Storgaard H, Poulsen P, Saxena R, Ladd C, Schulze PC, Mazzini MJ, Jensen CB, Krook A, Bjornholm M, Tornqvist H, Zierath JR, Ridderstrale M, Altshuler D, Lee RT, Vaag A, Groop LC, Mootha VK. TXNIP regulates peripheral glucose metabolism in humans. PLoS Med. 2007; 4:e158. [PubMed: 17472435]

Raben DM, Baldassare JJ. A new lipase in regulating lipid mobilization: hormone-sensitive lipase is not alone. Trends Endocrinol Metab. 2005; 16:35–36. [PubMed: 15734142]

Russell L, Forsdyke DR. A human putative lymphocyte G0/G1 switch gene containing a CpG-rich island encodes a small basic protein with the potential to be phosphorylated. DNA Cell Biol. 1991; 10:581–591. [PubMed: 1930693]

Rydel TJ, Williams JM, Krieger E, Moshiri F, Stallings WC, Brown SM, Pershing JC, Purcell JP, Alibhai MF. The crystal structure, mutagenesis, and activity studies reveal that patatin is a lipid acyl hydrolase with a Ser-Asp catalytic dyad. Biochemistry. 2003; 42:6696–6708. [PubMed: 12779324]

Ryden M, Jocken J, van Harmelen V, Dicker A, Hoffstedt J, Wiren M, Blomqvist L, Mairal A, Langin D, Blaak E, Arner P. Comparative studies of the role of hormone-sensitive lipase and adipose

triglyceride lipase in human fat cell lipolysis. Am J Physiol Endocrinol Metab. 2007; 292:E1847–E1855. [PubMed: 17327373]

Schweiger M, Schoiswohl G, Lass A, Radner FP, Haemmerle G, Malli R, Graier W, Cornaciu I, Oberer M, Salvayre R, Fischer J, Zechner R, Zimmermann R. The C-terminal region of human adipose triglyceride lipase affects enzyme activity and lipid droplet binding. J Biol Chem. 2008; 283:17211–17220. [PubMed: 18445597]

Smirnova E, Goldberg EB, Makarova KS, Lin L, Brown WJ, Jackson CL. ATGL has a key role in lipid droplet/adiposome degradation in mammalian cells. EMBO Rep. 2006; 7:106–113. [PubMed: 16239926]

Soni KG, Mardones GA, Sougrat R, Smirnova E, Jackson CL, Bonifacino JS. Coatomer-dependent protein delivery to lipid droplets. J Cell Sci. 2009; 122:1834–1841. [PubMed: 19461073]

Sztalryd C, Xu G, Dorward H, Tansey JT, Contreras JA, Kimmel AR, Londos C. Perilipin A is essential for the translocation of hormone-sensitive lipase during lipolytic activation. J Cell Biol. 2003; 161:1093–1103. [PubMed: 12810697]

Villena JA, Roy S, Sarkadi-Nagy E, Kim KH, Sul HS. Desnutrin, an adipocyte gene encoding a novel patatin domain-containing protein, is induced by fasting and glucocorticoids: ectopic expression of desnutrin increases triglyceride hydrolysis. J Biol Chem. 2004; 279:47066–47075. [PubMed: 15337759]

Watt MJ, Steinberg GR. Pathways involved in lipid-induced insulin resistance in obesity. Future Medicine. 2007; 2:659–667.

Watt MJ, Steinberg GR. Regulation and function of triacylglycerol lipases in cellular metabolism. Biochem J. 2008; 414:313–325. [PubMed: 18717647]

Zandbergen F, Mandard S, Escher P, Tan NS, Patsouris D, Jatkoe T, Rojas-Caro S, Madore S, Wahli W, Tafuri S, Muller M, Kersten S. The G0/G1 switch gene 2 is a novel PPAR target gene. Biochem J. 2005; 392:313–324. [PubMed: 16086669]

Zechner R, Kienesberger PC, Haemmerle G, Zimmermann R, Lass A. Adipose triglyceride lipase and the lipolytic catabolism of cellular fat stores. J Lipid Res. 2009; 50:3–21. [PubMed: 18952573]

Zimmermann R, Lass A, Haemmerle G, Zechner R. Fate of fat: the role of adipose triglyceride lipase in lipolysis. Biochim Biophys Acta. 2009; 1791:494–500. [PubMed: 19010445]

Zimmermann R, Strauss JG, Haemmerle G, Schoiswohl G, Birner-Gruenberger R, Riederer M, Lass A, Neuberger G, Eisenhaber F, Hermetter A, Zechner R. Fat mobilization in adipose tissue is promoted by adipose triglyceride lipase. Science. 2004; 306:1383–1386. [PubMed: 15550674]

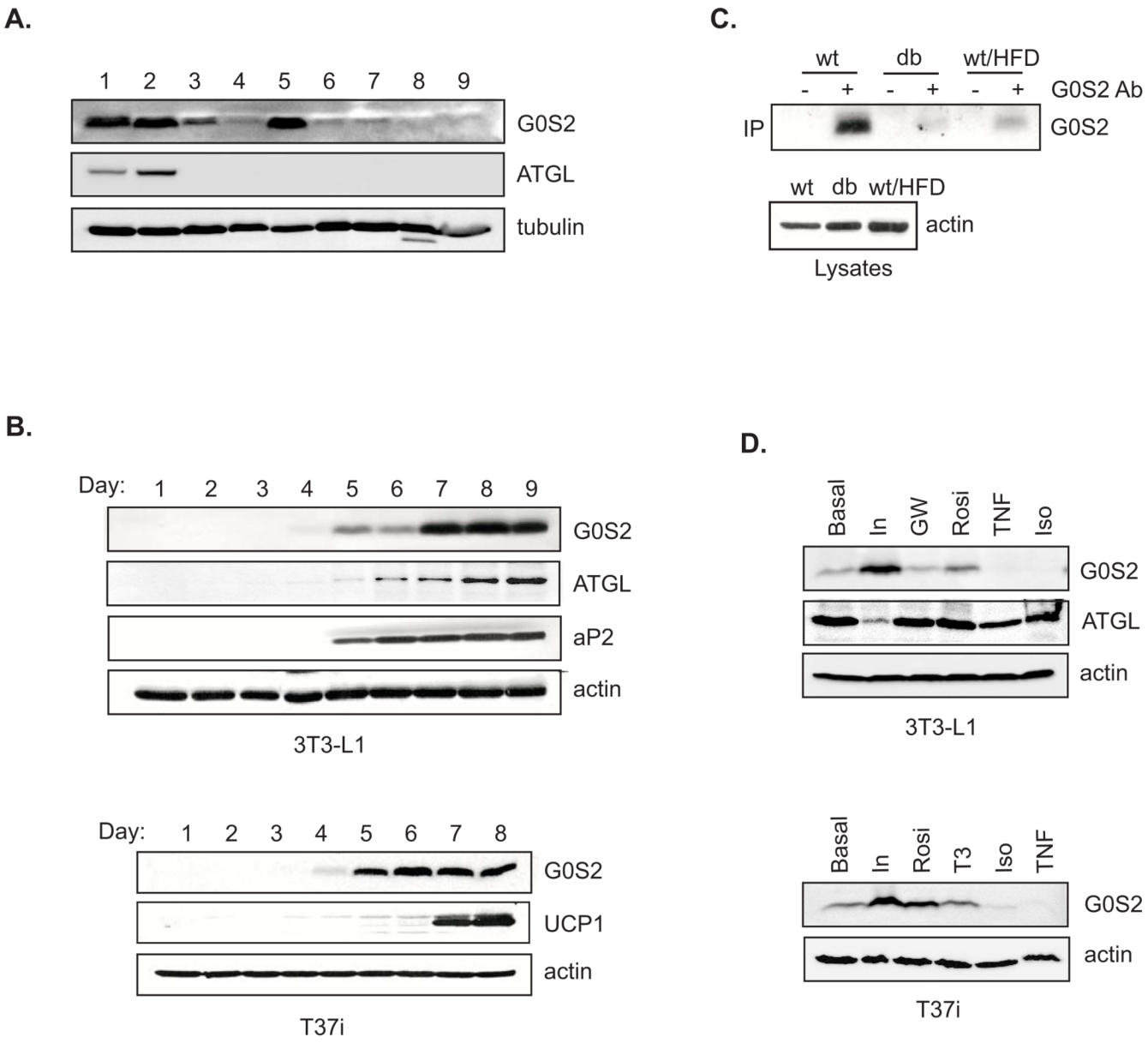

Figure 1. Regulation of G0S2 protein expression

A. Tissue distribution of G0S2 protein by immunoblotting analysis. 1, epididymal white adipose tissue; 2, interscapular brown adipose tissue; 3, heart; 4, skeletal muscle (hindlimb, upper leg muscle); 5, liver; 6, lung; 7, spleen; 8, pancreas; 9, kidney. β-tubulin was used as a loading control. **B**. Expression of G0S2 protein was analyzed by immunoblotting in lysates from differentiated 3T3-L1 and T37i adipocytes. Day 1 represents undifferentiated preadipocytes. aP2 was used as an adipocytes differentiation marker. UCP1 was used as a brown adipocyte specific marker. β-actin was used as a loading control. **C**. Immunoprecipitation was performed in extracts (equal amount of total protein) of mouse epididymal adipose using either anti-G0S2 serum (+) or preimmune serum (−). G0S2 in the immunoprecipitates were analyzed by immunoblotting. Mice used are wild type mice (wt) and *db/db* mice on normal chow, and wild type mice fed with high fat diet for 8 weeks (wt/HFD). **D**. Following 4 hr serum deprivation, 3T3-L1 and T37i adipocytes were treated for 8

h with 50 nM insulin (In), 10 nM triiodothyronine (T3), 10 μM GW501516 (GW), 1 μM rosiglitazone (Rosi), 1 μM isoproterenol/0.25 mM IBMX (Iso) or 20 ng/ml TNFα in serum-free medium. Immunoblotting was performed to detect the levels of G0S2 in the cell lysates, using β-actin as a loading control.

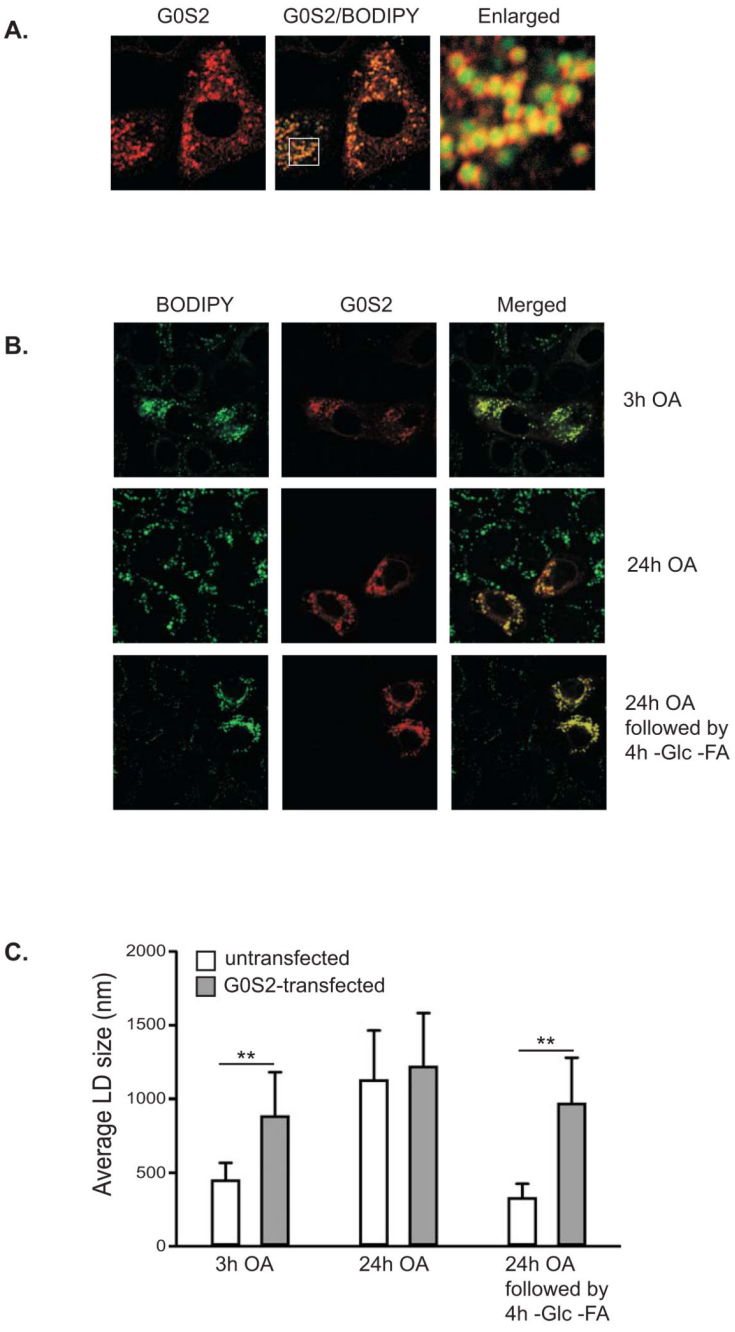

Figure 2. Overexpression of G0S2 inhibits lipid droplet degradation mediated by nutrient withdrawal

A. Immunofluorescence staining with anti-G0S2 antibodies was performed to reveal localization of overexpressed G0S2 in HeLa cells. Lipid droplets were co-stained with BODIPY 493/503 fluorescence dye. **B**. HeLa cells transiently expressing G0S2 were incubated under normal growth conditions with 400 μM of oleic acid complexed to albumin at a molar ratio of 8:1 for 3 h (upper panel) or 24 h (middle panel). A separate set of cells were incubated in serum-free and glucose-free medium for 4 h following 24 h of incubation with 400 μM of oleic acid (lower panel). Immunofluorescence staining with anti-G0S2 antibodies was performed to reveal the transfected cells. Lipid droplets were co-stained with

BODIPY 493/503 fluorescence dye. **C**. Quantification of lipid droplet diameter. An average of 80 lipid droplets was measured for each point. Data are shown as mean ± SD, $^{**}p < 0.01$, *t*-test.

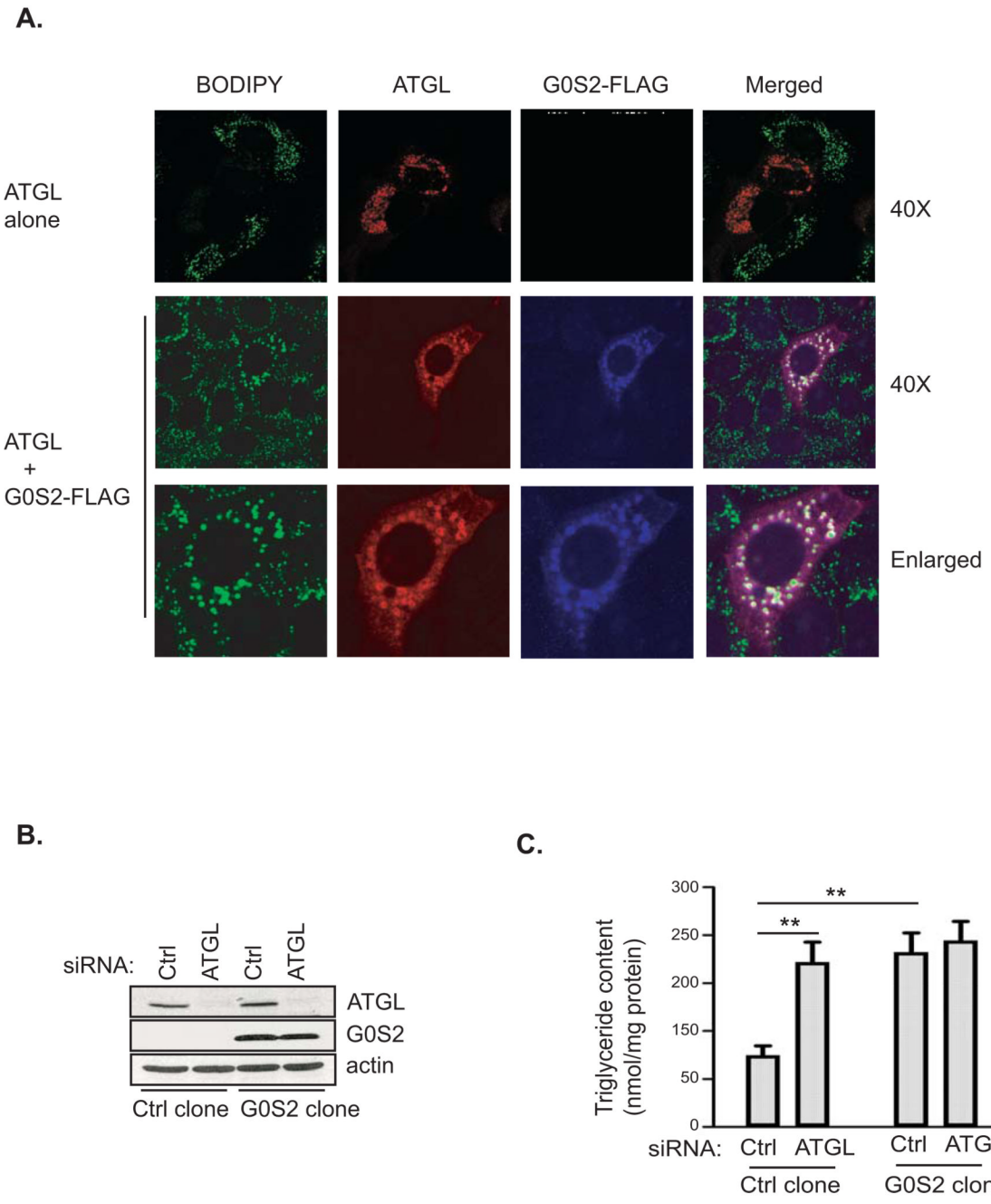

Figure 3. G0S2 inhibits lipid droplet degradation mediated by ATGL

A. HeLa cells transfected with ATGL in the absence (upper panel) or presence (lower panel) of G0S2-FLAG were incubated under normal growth conditions with 400 μM of oleic acid complexed to albumin for 3 h. Immunofluorescence staining was performed by using anti-ATGL (red) and anti-FLAG (blue) antibodies. Lipid droplets were co-stained with BODIPY 493/503 fluorescence dye. **B & C**. Stable HeLa cell clones with or without untagged G0S2 expression were treated with ATGL siRNA (ATGL KD) or control mismatch siRNA (Ctrl KD). Protein expression was analyzed by immunoblotting with anti-ATGL and anti-G0S2 antibodies **(B)**. The cells were incubated in 400 μM of oleic acid for 3 h and the intracellular

TAG content was determined as described in *Materials and Methods*. The data were normalized with the total protein amounts in the cell extracts (C) (data are shown as mean ± SD and represent three independent experiments, **$p < 0.01$, *t*-test).

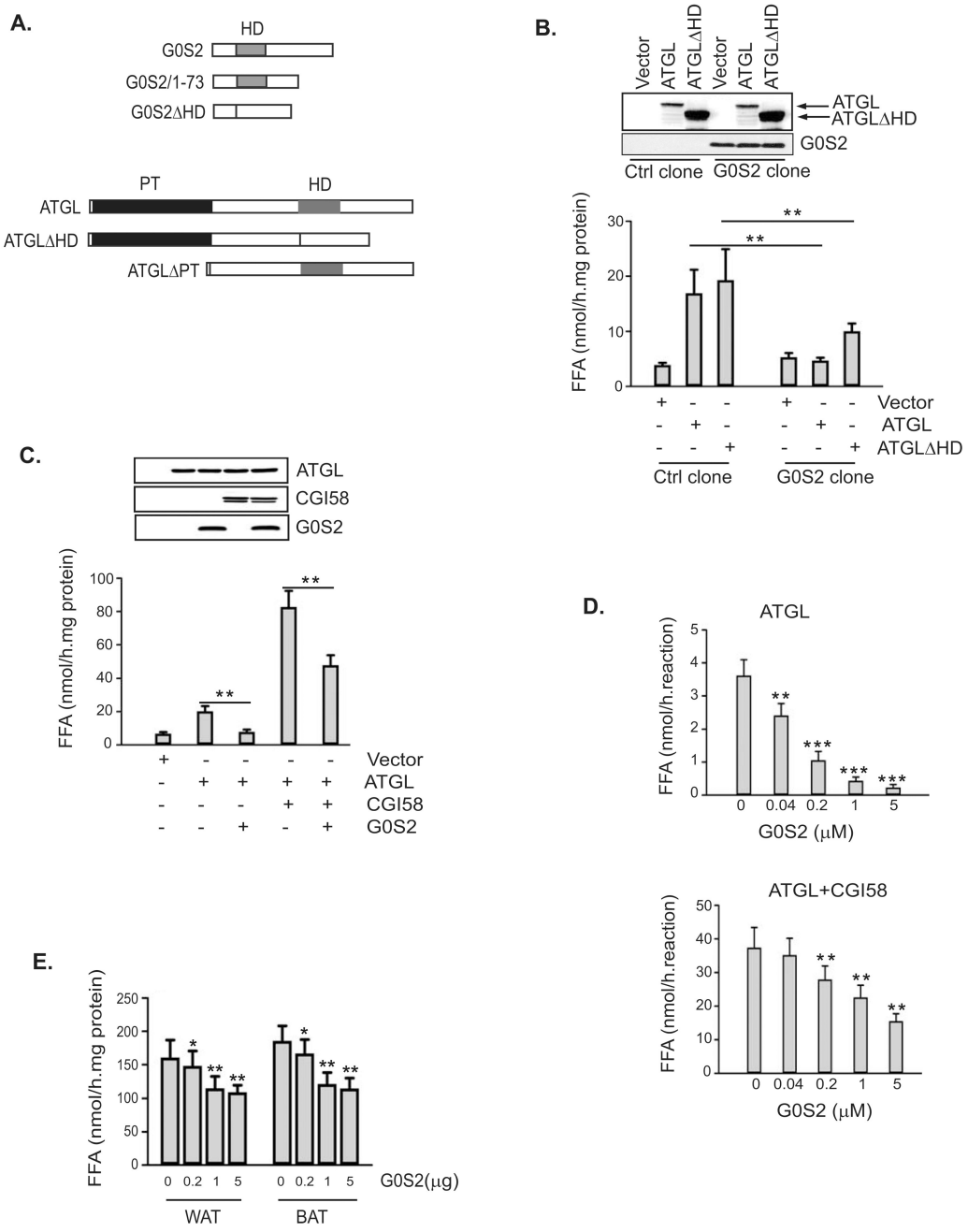

Figure 4. G0S2 selectively inhibits the TAG hydrolase activity of ATGL

A. Schematic structures of generated mutants of murine G0S2 and ATGL. The location of the hydrophobic domain (HD) in both proteins is indicated as gray bars, and the patatin domain (PT) in ATGL is indicated by a black region. **B**. HeLa cells from control clone or G0S2-expressing clone were transfected with vector alone, ATGL, ATGLΔHD. 24 h after transfection, ATGL and G0S2 proteins were detected with anti-ATGL and anti-G0S2 antibodies in immunoblotting using cell extracts. TAG hydrolase activity in cell extracts was measured using ^{3}H-labeled triolein as substrate, and was normalized with the total protein levels of the cell extracts. **C**. Extracts of HeLa cells singly expressing ATGL, CGI-58 or

G0S2 were mixed in various combinations, and TAG hydrolase activity was determined. Proteins in parallel mixtures were revealed in immunoblotting. **D**. ATGL and CGI-58 produced by using *in vitro* translation system were mixed with increasing amounts of purified recombinant G0S2, and were subjected to TAG hydrolase activity assays. **E**. Increasing amounts of recombinant purified G0S2 was added to extracts (100 μg total protein) of epididymal (WAT) and interscapular (BAT) fat tissue, and TAG hydrolase activity was determined.

All data are shown as mean ± SD and represent three independent experiments, $*p < 0.05$, $**p < 0.01$, $***p < 0.001$, *t*-test.

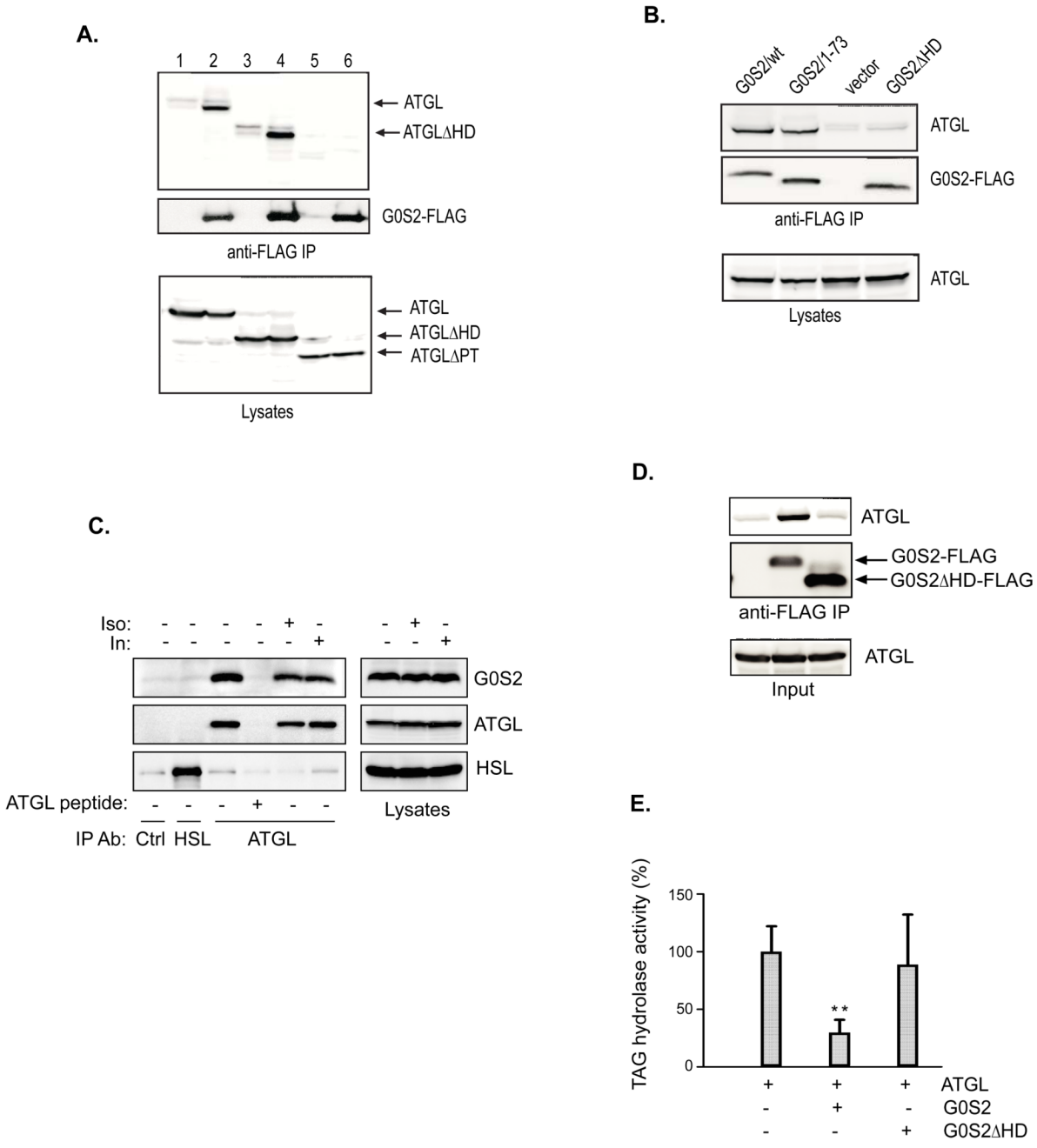

Figure 5. G0S2 specifically interacts with ATGL

A. HeLa cells were co-transfected with vector alone or G0S2-FLAG together with different ATGL constructs (1, ATGL+vector; 2, ATGL+G0S2-FLAG; 3, ATGLΔHD+vector; 4, ATGLΔHD+G0S2-FLAG; 5, ATGLΔPT+vector; 6, ATGLΔPT+G0S2-FLAG). G0S2-FLAG proteins were immunoprecipitated with anti-FLAG antibodies. G0S2 and ATGL proteins in immunoprecipitates and lysates were detected by immunoblotting with FLAG and ATGL antibodies. **B**. HeLa cells were co-transfected with wild type ATGL along with vector alone or various G0S2-FLAG constructs. Immunoprecipitation and immunoblotting analysis were performed as described in **A. C**. 3T3-L1 adipocytes were pretreated with or

without 1 μM isoproterenol or 100 nM insulin for 30 min. Immunoprecipitation of endogenous ATGL was performed in the lysates in the presence or absence of an ATGL epitope-blocking peptide. Nonspecific control and HSL antibodies were used as controls. G0S2, ATGL and HSL in precipitates and lysates were analyzed by immunoblotting with respective antibodies. **D**. Anti-FLAG immunoprecipitation was performed following the *in vitro* transcription/translation reactions. ATGL and FLAG-tagged G0S2 proteins in precipitates were analyzed by immunoblotting with anti-ATGL and anti-FLAG antibodies. **E**. The TAG hydrolase activity in the cell extracts was measured using ^{3}H-labeled triolein as substrate. The activity was normalized with the total protein levels of the cell extracts, and is shown in relation to basal activity detected in vector-transfected cells from the control clone. Data are shown as mean ± SD and represent three independent experiments, $^{**}p < 0.01$, *t*-test.

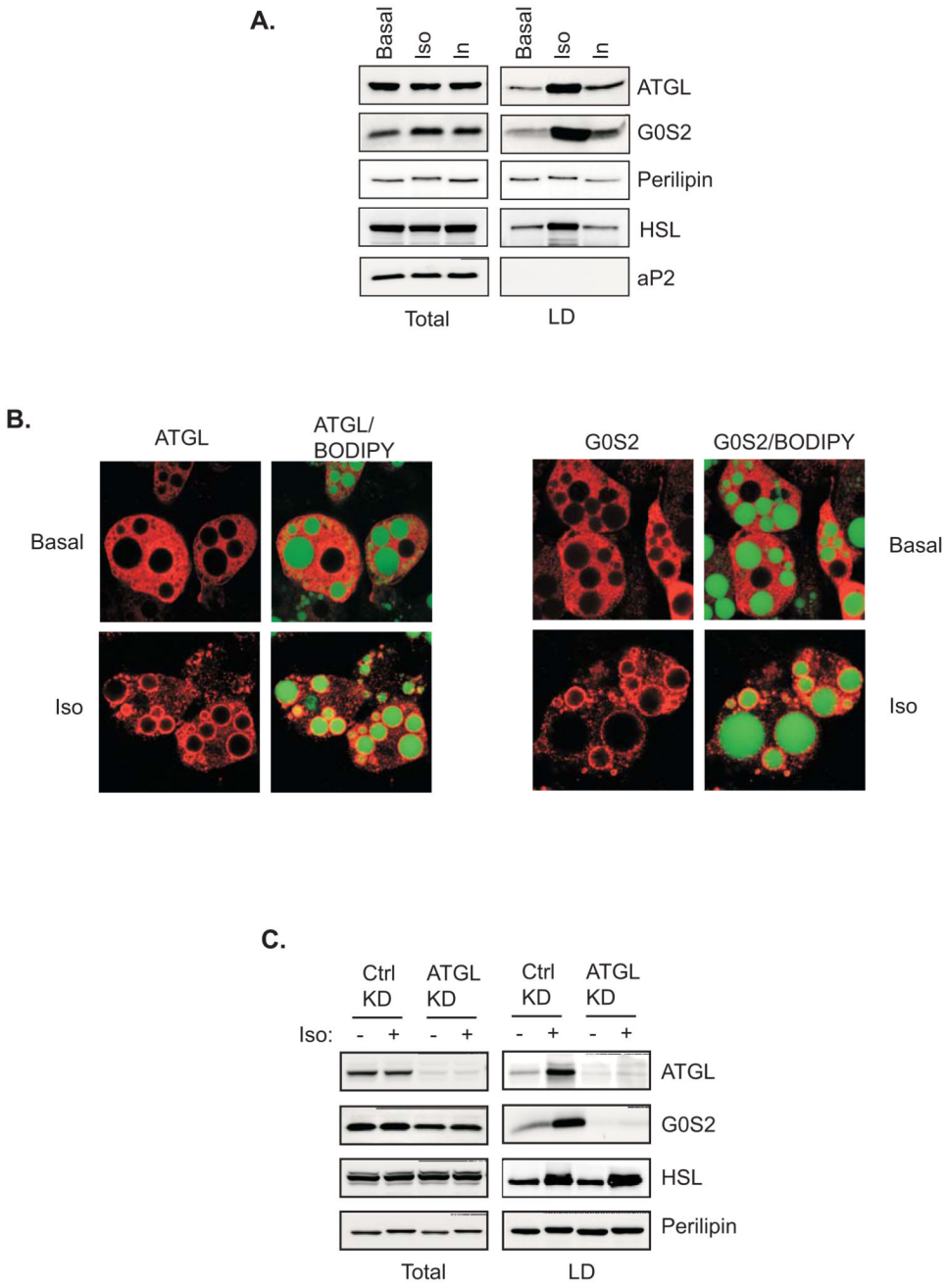

Figure 6. Lipid droplet localization of ATGL and G0S2 in adipocytes

A. 3T3 L1 adipocytes were treated with or without 1μM isoproterenol or insulin for 30 min. Lipid droplets were isolated by ultracentrifugation. Total and lipid droplet-associated proteins were subjected to immunoblotting using antibodies against ATGL, perilipin, HSL, G0S2 and aP2. **B**. Immunofluorescence staining with anti-ATGL antibodies was performed to reveal localization of endogenous ATGL in 3T3-L1 adipocytes pretreated with or without 1 μM isoproterenol/0.25 mM IBMX for 30 min. Lipid droplets were co-stained with BODIPY 493/503. **C**. siRNA-mediated knockdown was performed by electroporating 3T3-L1 adipocytes with either control siRNA (Ctrl) or ATGL-specific siRNA (KD). 3 days later,

cells were treated with or without 1 μM isoproterenol for 30 min followed by lipid droplets isolation. Total and lipid droplet-associated levels of ATGL, HSL, G0S2 and perilipin were analyzed by immunoblotting.

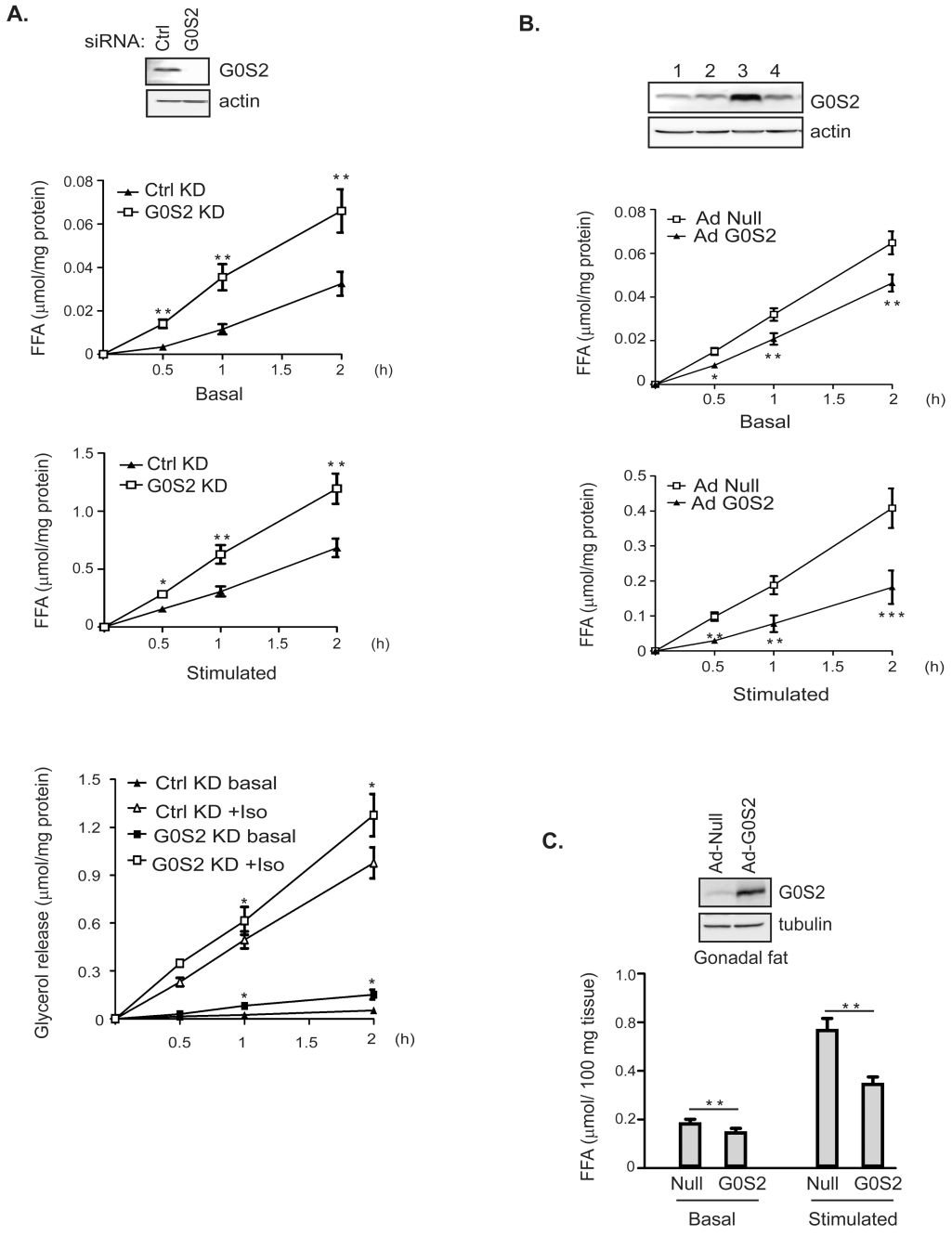

Figure 7. G0S2 attenuates basal and stimulated lipolysis in adipocytes

A. siRNA-mediated knockdown of G0S2 in 3T3-L1 adipocytes was achieved by electroporating cells with either control siRNA or G0S2-specific siRNA. Cells were treated 3 days later with (stimulated) or without (basal) 1 μM isoproterenol for 30 min, 60 min and 2 h. Basal and stimulated FFA and glycerol release were measured and normalized with the total protein levels in the cell extracts. Expression of G0S2 protein was analyzed by immunoblotting, using β-actin as a loading control. Data are shown as mean ± SD and represent three independent experiments, $*P < 0.05$, $**P < 0.01$, one-way ANOVA. **B**. Overexpression of G0S2 in 3T3-L1 adipocytes was achieved by infecting cells with

recombinant adenovirus encoding murine G0S2 (Ad-G0S2). A null virus was used as a control. G0S2 expression was analyzed by immunoblotting 3 days after infection: 1, null virus at high dosage; 2, null virus at low dosage; 3, Ad-G0S2 at high dosage; 4, Ad-G0S2 at low dosage. 3 days following infection with either null or Ad-G0S2 at high dosage, lipolysis of 3T3-L1 adipocytes was measured as described in **A**. Data are shown as mean ± SD and represent three independent experiments, $*P < 0.05$, $**P < 0.01$, $***P < 0.001$, one-way ANOVA. **C**. Overexpession of G0S2 in gonadal fat explants was achieved by infection with Ad-G0S2 using null virus as a control. 2 days post infection explants were treated with (stimulated) or without (basal) 1 μM isoproterenol for 2 h. Basal and stimulated FFA release was measured and normalized with the total mass of explants. Data are shown as mean ± SD and represent three independent experiments, $**P < 0.01$, *t*-test.

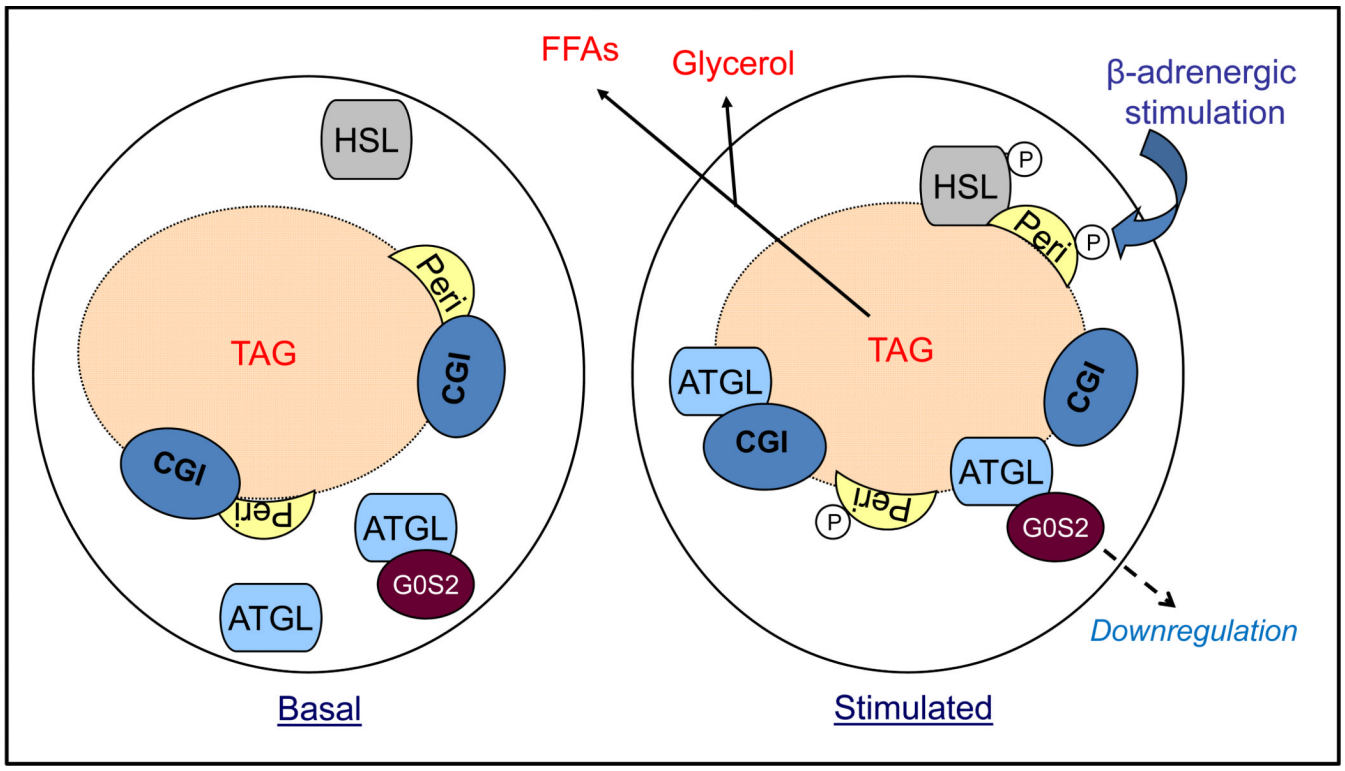

Figure 8. Model for the regulation of adipose lipolysis by G0S2

Under basal conditions when the lipolytic rate is very low, ATGL is mostly localized in ER-related membranes in the cytoplasm. At least a small fraction of ATGL is in complex with G0S2. Upon β-adrenergic stimulation, PKA activation results in phosphorylation of perilipin A at multiple sites. Consequently, ATGL, both G0S2-bound and –unbound form, undergoes translocation onto lipid droplets. Translocation of unbound ATGL along with HSL leads to acute activation of TAG hydrolysis. Prolonged β-adrenergic stimulation subsequently downregulates protein level of G0S2, thereby releasing more ATGL for sustained lipolysis.